

## TITLE

A Millimeter-Scale Change in Leaf Litter Placement Within Soil-Water Interfaces Alters Carbon Dioxide and Methane Emission

## AUTHORS

Hao Liu <sup>a,c</sup>, Yining Zhang <sup>b</sup>, Yujia Cai <sup>a,d</sup>, Ziyang Liu <sup>a,e</sup>, Liang Li <sup>a</sup>, Yaqin Wang <sup>a,d</sup>, Xiao Shu <sup>a,d</sup>, Royston Goodacre <sup>c</sup>, Zheng Chen <sup>a,\*</sup> (Email address: zheng.chen@xjtlu.edu.cn)

<sup>a</sup> Department of Health and Environmental Sciences, Xi'an Jiaotong-Liverpool University, Suzhou 215123, Jiangsu Province, China

<sup>b</sup> Department of Biological Sciences, Xi'an Jiaotong-Liverpool University, Suzhou 215123, Jiangsu Province, China

<sup>c</sup> Centre for Metabolomics Research, Department of Biochemistry, Cell and Systems Biology, Institute of Systems, Molecular and Integrative Biology, University of Liverpool, Liverpool L697BE, United Kingdom

<sup>d</sup> Department of Geography & Planning, School of Environmental Sciences, University of Liverpool, Brownlow Hill, Liverpool L697ZX, United Kingdom

<sup>e</sup> Department of Chemistry, University of Liverpool, Crown Street, Liverpool, L697ZD, United Kingdom

## CORRESPONDENCE AUTHOR

Zheng Chen

Email: [Zheng.chen@xtjlu.edu.cn](mailto:Zheng.chen@xtjlu.edu.cn)

## STATEMENT

This preprint has been submitted to the journal Soil Biology and Biochemistry (manuscript number: SBB25696 ) for peer review.

### **Highlights**

- The placement of leaf litter at SWI significantly impacts on CO<sub>2</sub> and CH<sub>4</sub> emissions from wetland soils.
- A thin soil layer covering leaf litter led to doubled soil CH<sub>4</sub> emissions and a 25% reduction in CO<sub>2</sub> emissions, and an overall lower GWP20, compared to leaf litter without soil covering.
- The presence or absence of a thin soil covering on leaf litter triggers distinct biogeochemical processes, influencing CO<sub>2</sub> and CH<sub>4</sub> emissions
- Geographic patterns, particularly the spatial distribution of plant litters along the soil redox gradient, are crucial factors in controlling carbon fate

1 **Title**

2 A Millimeter-Scale Change in Leaf Litter Placement Within Soil-Water Interfaces Alters Carbon Dioxide and  
3 Methane Emission

4 **Authors**

5 Hao Liu <sup>a,c</sup>, Yining Zhang <sup>b</sup>, Yujia Cai <sup>a,d</sup>, Ziyang Liu <sup>a,e</sup>, Liang Li <sup>a</sup>, Yaqin Wang <sup>a,d</sup>, Xiao Shu <sup>a,d</sup>, Royston Goodacre <sup>c</sup>,  
6 Zheng Chen <sup>a,\*</sup> (Email address: zheng.chen@xjtlu.edu.cn)

7 <sup>a</sup> Department of Health and Environmental Sciences, Xi'an Jiaotong-Liverpool University, Suzhou 215123,  
8 Jiangsu Province, China

9 <sup>b</sup> Department of Biological Sciences, Xi'an Jiaotong-Liverpool University, Suzhou 215123, Jiangsu Province,  
10 China

11 <sup>c</sup> Centre for Metabolomics Research, Department of Biochemistry, Cell and Systems Biology, Institute of  
12 Systems, Molecular and Integrative Biology, University of Liverpool, Liverpool L697BE, United Kingdom

13 <sup>d</sup> Department of Geography & Planning, School of Environmental Sciences, University of Liverpool, Brownlow  
14 Hill, Liverpool L697ZX, United Kingdom

15 <sup>e</sup> Department of Chemistry, University of Liverpool, Crown Street, Liverpool, L697ZD, United Kingdom

16 **Abstract**

17 Flooded soils play a critical role in global carbon cycling, serving as significant reservoirs of soil organic carbon  
18 and sources of carbon emissions. Leaf litter, particularly from local vegetation, is a major contributor to soil  
19 organic carbon formation in these ecosystems, with its decomposition driving the production of carbon dioxide  
20 and methane. While numerous studies have investigated the factors influencing leaf litter decomposition and  
21 the associated greenhouse gas emissions, the impact of millimeter-scale variations in leaf litter placement

22 within the soil-water interface (SWI) remains underexplored. This study hypothesizes that such minor changes  
23 in burial depth can significantly alter the emission patterns of CO<sub>2</sub> and CH<sub>4</sub>. To test this, a microcosm  
24 experiment was conducted, monitoring gas fluxes and profiles of physicochemical properties in treatments  
25 with leaf litter closely placed at two depths within the SWI. Results revealed that a sub-centimeter difference  
26 in leaf litter placement could lead to a substantial shift in CO<sub>2</sub> and CH<sub>4</sub> emissions, with important implications  
27 for modeling wetland carbon dynamics and predicting their climate impact. These findings underscore the  
28 sensitivity of greenhouse gas emissions to small-scale environmental variations, highlighting the need for more  
29 precise models in estimating wetland contributions to global carbon fluxes.

## 30 **1. Introduction**

31 Wetlands are important reservoirs of soil organic carbon as well as sources of carbon emission (Xiao et al.,  
32 2019). While wetlands cover only 5-8% of the global terrestrial area, wetland soils contain about 20-25% of  
33 global soil carbon stocks (Mitra, 2005; Mitsch et al., 2012; Nahlik and Fennessy, 2016). The plant litters from  
34 local vegetation contribute significantly to the soil organic carbon (SOC) formation (Cao et al., 2020;  
35 Scharlemann et al., 2014) while the leaf litter have greater impacts on SOC accumulation than stem and root  
36 litter in forested wetlands (Ding et al., 2023; Ji et al., 2020). Leaf litter is an important carbon source for forested  
37 wetland ecosystems, and its decomposition process affects the entire ecosystem (Stoler and Relyea, 2010;  
38 Stoler and Relyea, 2013; Watkins et al., 2011). The carbon and nutrients released from leaf litter fuels the  
39 respiration of microbes and methanogenesis in wetlands, which converts the labile carbon released from leaf  
40 litter into carbon dioxide and methane (Corteselli et al., 2017; Dušek et al., 2020). The linkage between leaf  
41 litter decomposition and greenhouse gases emission have been extensively studied for wetlands. The factors  
42 like leaf species (Yakimovich et al., 2018; Yavitt and Williams, 2015), hydroperiod (Batson et al., 2015; Battle  
43 and Golladay, 2001; Neiff et al., 2006; Peng et al., 2022), temperature (Bridgham et al., 2006; Ma et al., 2022),  
44 oxygen availability (Dušek et al., 2020; Neckles and Neill, 1994), water chemistry (Chiapponi et al., 2024) are  
45 found to collectively influence decomposition rate of leaf litter in various types of wetlands, therefore

46 controlling the CO<sub>2</sub> and CH<sub>4</sub> emission. However, to date the positioning of fresh leaf litter has been rarely  
47 discussed and knowledge of its impact on wetland CO<sub>2</sub> and CH<sub>4</sub> emission remains scarce.

48 The placement of leaf litter in soil significantly influences decomposition rates and the emission of CO<sub>2</sub> and CH<sub>4</sub>.  
49 Factors such as burial depth, soil-litter mixing, and the removal of aboveground litter affect leaf litter  
50 processing in wetlands (Gong et al., 2020; Hu et al., 2021; Ma et al., 2022). Decomposition is most rapid near  
51 the wetland surface, where freshly deposited litter and newly synthesized labile organic matter are abundant  
52 (Schiff et al., 1998). This surface oxic layer is also the primary site for CO<sub>2</sub> and CH<sub>4</sub> production (Kayranli et al.,  
53 2009). However, the variable positions of leaf litter and dynamic conditions in natural wetlands create  
54 challenges in accurately determining CO<sub>2</sub> and CH<sub>4</sub> emissions from litter decomposition at different locations  
55 along the soil-water interface (SWI).

56 The ratio of CO<sub>2</sub> and CH<sub>4</sub> emitted from wetlands during leaf litter decomposition are primarily influenced by  
57 redox condition (Dušek et al., 2020; Galera et al., 2023; Nilsson and Öquist, 2009). CO<sub>2</sub> emission dominates the  
58 wetland emission in dry period and aerobic layer of wetland soils whereas CH<sub>4</sub> emission becomes more  
59 significant in the oxygen-depleted cases like high water table and anaerobic soil layer (Bridgham et al., 2013;  
60 Ding et al., 2002; Liu et al., 2021). Nonetheless, the transition from oxic to anoxic zone usually occurs over a  
61 depth ranging from several millimeters to centimeters below SWIs (Glud et al., 2007; Roy et al., 2004). The  
62 sharp redox gradient suggests that a minor displacement of leaf litter at the SWIs may change the patterns of  
63 CO<sub>2</sub> and CH<sub>4</sub> fluxes a lot, but this effect has not to the best of the authors knowledge been previously described.  
64 Hereby, we propose that the partitioning of CO<sub>2</sub> and CH<sub>4</sub> is sensitive to a millimeter scale variation in leaf litter  
65 burial depth across the SWIs.

66 This study hypothesizes that the positioning of leaf litter in the SWI significantly affects the fate of dissolved  
67 organic carbon. We think that even slight variations in burial depth, less than ten millimeters, can alter CO<sub>2</sub> and  
68 CH<sub>4</sub> emission patterns from wetlands, complicating model predictions. To investigate this, we conducted a  
69 microcosm experiment, monitoring CO<sub>2</sub> and CH<sub>4</sub> emissions after adding leaf litter at two closely positioned  
70 locations. Concurrently, we measured the profiles of dissolved oxygen (DO), redox potential (Eh), fluorescent

71 dissolved organic matter (fDOM) and microbial communities across different treatments. The results could  
72 improve the accuracy of models estimating CO<sub>2</sub> and CH<sub>4</sub> emissions from wetlands.

## 73 **2. Materials and methods**

### 74 **2.1. Collection of soil, water, and leaf litter**

75 A rice paddy soil was collected from a farmland in Kunshan, Jiangsu Province, China. The soil was air-dried  
76 under room temperature. The gravel and plant litter were removed from the soil with a one-millimeter mesh  
77 sieve. The surface water was collected from a local pond. The water was filtered with 0.45 µm filter cartridge  
78 and then autoclaved. The sterile surface water was stored in 1-L Schott bottle < 4°C before use. The fresh leaf  
79 litter from *Liriodendron Chinense* was collected in campus and stored in a sterile plastic bag before use.

### 80 **2.2. Microcosm experiment**

81 Open-top microcosms were constructed using collected paddy soil and surface water. Each microcosm  
82 consisted of a soil column measuring 60 mm in height and a water column of 30 mm. These structures were  
83 then incubated at room temperature (~20 °C). To offset evaporation, ultrapure water was added daily  
84 throughout the incubation and experimental period.

85 To test the hypothesis, three experimental groups were established. The first group received dry uncovered  
86 (denoted as LU), with the leaf litter placed at the soil-water interface (SWI). The second group was treated with  
87 covered leaf litter (LC), where the leaf litter was covered with a 10-mm-thick soil layer. A control group with  
88 leaf litter addition (NL) was included. Each group was replicated twice. For both the LU and LC groups, 0.8 g of  
89 dry leaf litter were added to the water column, and after ~4 h, the leaf litter settled at the SWI. In the LC group,  
90 a stainless steel spatula was used to gently till the topsoil, covering the leaf litter with a roughly 10-mm thick  
91 layer.

92 Gas fluxes of carbon dioxide and methane were monitored at 0, 5, and 15 h post-leaf litter addition, and

93 subsequently, measurements were continued on a daily basis. DO, Eh, fluorescent fDOM, and nitrogen species  
94 were analyzed on days 3, 14, and prior to the treatment. The porewater samples were collected using the  
95 Integrated Porwater Injection (IPI) samplers with a depth resolution of 2 mm (Yuan et al., 2019; Zhang et al.,  
96 2023).

### 97 **2.3. Measurement of CO<sub>2</sub> and CH<sub>4</sub> fluxes**

98 The real time concentration of carbon dioxide and methane was monitored using the LI-7810 trace gas analyzer  
99 (LI-COR, USA) and the closed dynamic chamber on daily basis. Every measurement takes 90 s, and the readings  
100 are fitted with a linear line. The slope of linear fitting line is the approximate emission rate and used to calculate  
101 the gas fluxes. A more detailed description of the chamber measurement is provided in the supplementary  
102 information. The global warming potential over a 20-year timescale (GWP20) is calculated after the AR6, with  
103 a factor of 81 chosen for biogenic methane (IPCC, 2021).

### 104 **2.4. fDOM characterization**

105 The excitation-emission matrix (EEM) of the sterile and filtered surface water and leaf litter leachate was  
106 characterized with Cary Eclipse fluorescence spectrometer (Agilent Technologies, USA). The EEM program  
107 parameters are as follows: scanned excitation from 200 to 450 nm every 5 nm at a rate of 1200 nm/min;  
108 detected emission from 300 to 550 nm with a slit width of 10 nm; the voltage of photomultiplier at 700 V.

109 The fluorescent components of dissolved organic matters in overlying water and porewater samples was  
110 analyzed using the 1260 Infinity high performance liquid chromatography (HPLC) system (Agilent Technologies,  
111 USA) equipped with a fluorescence detector (FLD) and a diode array detector (DAD). An autosampler injected  
112 a 5 µL aliquot of each sample. A gradient elution program of acetonitrile and 10 mM sodium acetate aqueous  
113 buffer is modified from a previous work (Li et al., 2013). Based on the EEM results, the parameters of FLD and  
114 DAD were optimized as follows: for FLD excitation at 207, 230, 315 nm, emission at zero order; for DAD  
115 absorption at 254 nm as proxy of aromatic compounds.

116 **2.5. *In situ* measurement of DO and Eh**

117 The dissolved oxygen and redox potential were profiled with commercially available (EasySensor, China) and  
118 self-made microelectrodes. The microelectrodes are mounted on the coordinate measuring system (see  
119 Section 2.4) and connected to CHI 1040 potentiostat (Chenhua Instrument, China). Each profile starts at 20 mm  
120 above the soil-water interface and ends at forty-millimeter below the interface. The readings were logged  
121 every 2 mm with a 30 s cycle.

122 **2.6. Nucleic acid extraction**

123 By end of the incubation, the water layer was collected into 50 mL sterile centrifuge tubes. The soil cores were  
124 collected in headless 5 mL syringe using the core sampling tool (see Section 2.5) and then sealed with parafilm.  
125 Both water samples and soil cores were frozen at  $-40\text{ }^{\circ}\text{C}$  immediately after collection. For each replicate, 150  
126 mm water samples were thawed and filtered through the sterile  $0.22\text{ }\mu\text{m}$  mixed cellulose esters membranes.  
127 The soil cores were segmented in 3 mm thick aliquot. Each soil aliquot was directly transferred into a 2 mm  
128 cryotube and weighed. The DNA from water and soil were extracted with the FastDNA Spin Kit (MP Biomedical,  
129 USA). The size of genomic DNA was verified using agarose gel electrophoresis. The DNA quality and  
130 concentration was determined using Nanodrop and Qubit (Thermo Fisher Scientific, USA).

131 **2.7. qPCR**

132 Each PCR reaction was carried out in  $20.0\text{ }\mu\text{L}$  mixture and contained  $1.0\text{ }\mu\text{L}$  DNA template,  $10.0\text{ }\mu\text{L}$  TB Green  
133 Premix Ex Taq (Tli RNaseH Plus) (Takara Bio, RR420A),  $1.0\text{ }\mu\text{L}$  of each primer ( $10\text{ }\mu\text{M}$ ), and nuclease-free water.  
134 The primer pairs were chosen for the V4 region of 16S rRNA gene (515F: 5'GTGCCAGCMGCCGCGTAA3', 806R:  
135 5'GGACTACHVGGGTWTCTAAT3'). The qPCR reactions were performed in triplicate under thermal cyler  
136 conditions of 15 min at  $95\text{ }^{\circ}\text{C}$ , and 39 cycles of 10 s at  $95\text{ }^{\circ}\text{C}$ , 30 s at  $55\text{ }^{\circ}\text{C}$  and 32 s at  $72\text{ }^{\circ}\text{C}$  in a 96-well format  
137 LightCycler 480 Real-Time PCR System (Roche). All results were normalized and calculated using the  $\Delta\text{Ct}$   
138 method.



## 139 **2.8. Amplicon sequencing and analysis**

140 The V3-V4 region of 16S ribosomal RNA gene was amplified using the primer pairs 341F  
141 (5'CCTACGGGAGGCAGCAG3') and 806R (5'GGACTACHVGGGTWTCTAAT3'). The length of amplified region is  
142 roughly 470 bp. The sequences were obtained on the NovaSeq 6000 platform (Illumina, USA) with a 2x250 bp  
143 paired-end run. The raw sequence files will be later deposited in an online archive.

144 The raw sequencing data was denoised and merged using the DADA2 pipeline (Callahan et al., 2016). The  
145 taxonomy of the amplicon sequence variants was assigned using QIIME2 and the latest SILVA database (Bolyen  
146 et al., 2019; Quast et al., 2013). The metabolic functional potential of the microbial communities was predicted  
147 using PICRUSt2 pipeline (Barbera et al., 2019; Douglas et al., 2020; Louca and Doebeli, 2018; Ye and Doak,  
148 2009).

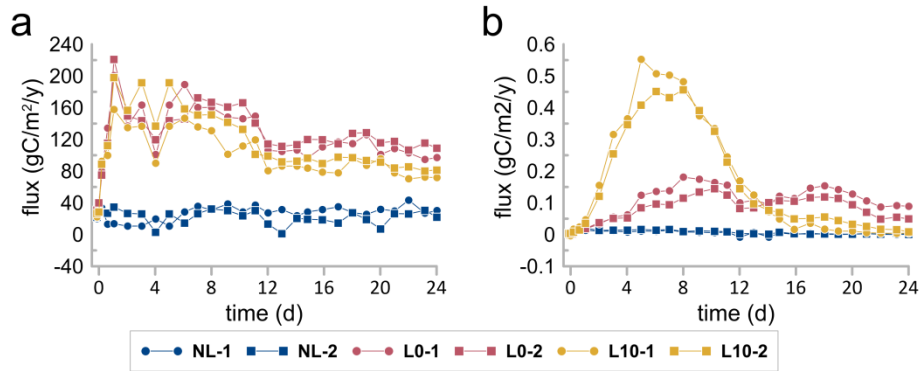
## 149 **3. Results**

### 150 **3.1. Temporal variation in CH<sub>4</sub> and CO<sub>2</sub> fluxes**

151 The CH<sub>4</sub> fluxes from the flooded soils were monitored from the treatments with or without the leaf litter  
152 amendment (Fig. 1a). Clear distinctions in CH<sub>4</sub> flux patterns were observed between the LU and LC groups,  
153 while the NL group released nearly no CH<sub>4</sub>. In the LC group, CH<sub>4</sub> fluxes increased immediately after amendment  
154 and peaked at an emission rate of 0.52-0.76 gC/m<sup>2</sup>/y on day 5. These fluxes remained around 0.6 gC/m<sup>2</sup>/y until  
155 day 8 and then diminished to almost zero by day 21. In contrast, the CH<sub>4</sub> flux curve for the LU group exhibited  
156 a more gradual increase, reaching a maximum intensity of 0.2 gC/m<sup>2</sup>/y on day 8, approximately one-fourth of  
157 the LC group's peak.

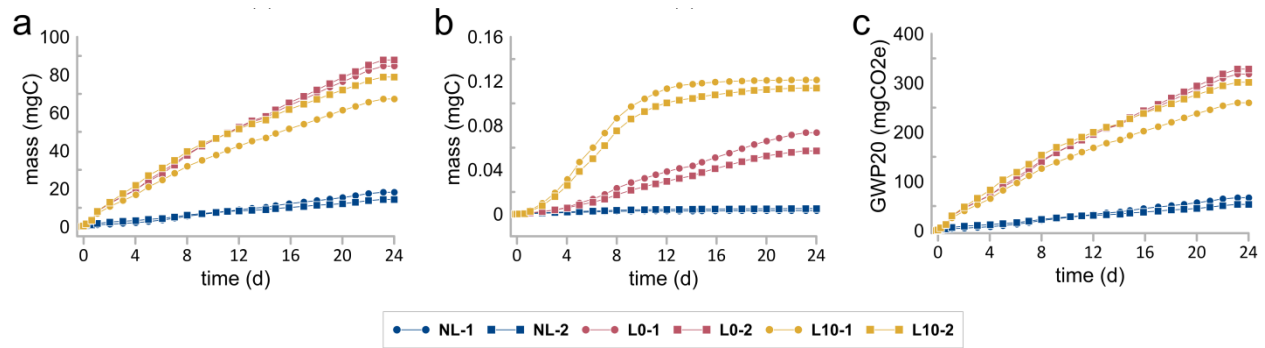
158 The CO<sub>2</sub> fluxes for the LU and LC groups exhibited similar trends (Fig. 1b). Both groups experienced an initial  
159 peak in CO<sub>2</sub> fluxes, reaching levels between 157 and 221 gC/m<sup>2</sup>/y in day 1. From day 2 to day 11, the intensity  
160 of CO<sub>2</sub> fluxes declined and fluctuated between 101 and 192 gC/m<sup>2</sup>/y, followed by a subsequent gradual  
161 decrease. Eventually, CO<sub>2</sub> fluxes leveled off within a range of 71 to 120 gC/m<sup>2</sup>/y, remaining stable until the 24-

162 day incubation period terminated. During this stage, the CO<sub>2</sub> fluxes in the LU group were, on average,  
 163 approximately 20% greater than those in the LC group. These distinct patterns in CH<sub>4</sub> fluxes and similar trends  
 164 in CO<sub>2</sub> fluxes were previously confirmed by replicated findings from an independent experiment (Fig. S1).



165  
 166 Fig. 1. (a) Temporal variations in CO<sub>2</sub> fluxes. (b) Temporal variations in CH<sub>4</sub> fluxes. The black arrows indicate the  
 167 points of profiling DO, Eh, fDOM in time. NL = control groups; LU = leaf litter placed at the soil-water interface;  
 168 LC = leaf litter was covered with a 10-mm-thick soil layer.

169 The overall cumulative CH<sub>4</sub> and CO<sub>2</sub> emissions are presented in Fig. 2. The LU and LC groups emitted 42.5 μgC  
 170 and 115.3 μgC of CH<sub>4</sub>, respectively (Fig. 2b). The LC group's CH<sub>4</sub> emissions were more than double those of the  
 171 LU group. Notably, the NL group did not emit any CH<sub>4</sub>, suggesting that CH<sub>4</sub> production is surely attributed to  
 172 the litter amendment. CO<sub>2</sub> emissions from the LU and LC groups were 103 mgC and 77 mgC, respectively, by  
 173 the end of the experiment (Fig. 3a). One centimeter repositioning of leaf litter resulted in a 25% reduction in  
 174 overall CO<sub>2</sub> emissions, reflecting the lower CO<sub>2</sub> fluxes during the late stage of incubation in the LC group. The  
 175 potential impact on climate change was assessed using the GWP20 metric (Fig. 3c) The GWP20 values for the  
 176 LU and LC groups were 323.3 mgCO<sub>2</sub>e and 280.7 mgCO<sub>2</sub>e, respectively. Despite the doubling of CH<sub>4</sub> emissions  
 177 due to leaf litter perturbation, the GWP20 of the LC group was still 13.2% lower than that of the LU group, due  
 178 to the reduced CO<sub>2</sub> release.



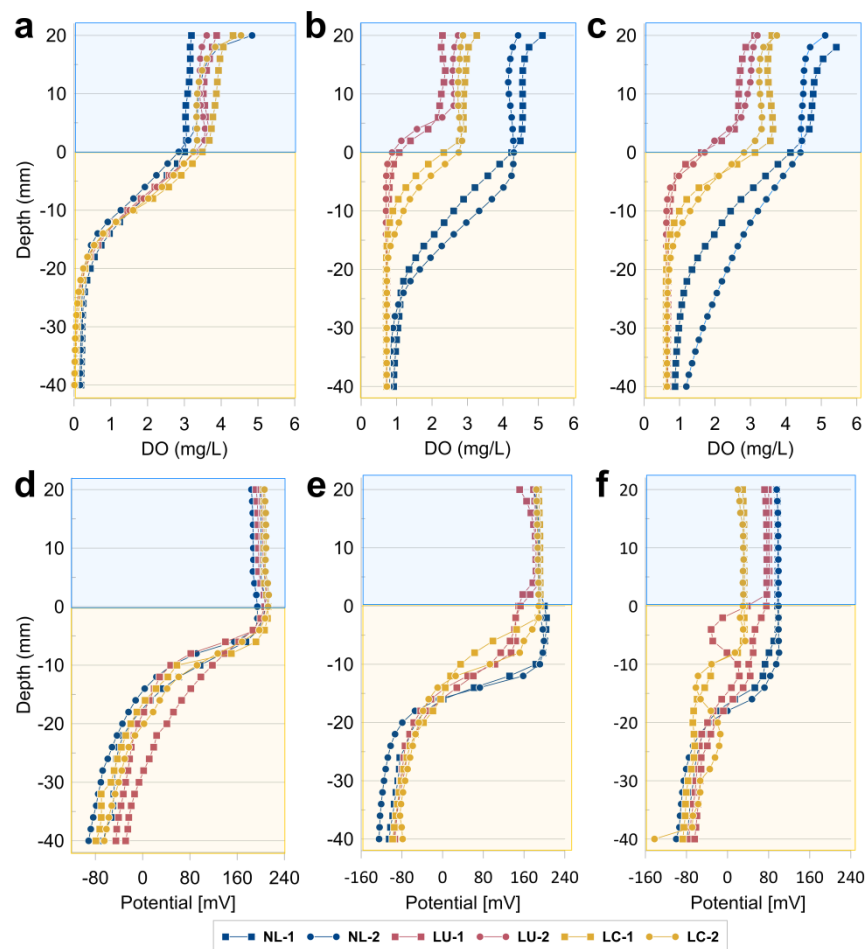
179  
 180 Fig. 2. (a) Cumulative carbon emission in the form of CO<sub>2</sub>. (b) Cumulative carbon emission in the form of CH<sub>4</sub>.  
 181 (c) The combined GWP20. NL = control groups; LU = leaf litter placed at the soil-water interface; LC = leaf litter  
 182 was covered with a 10-mm-thick soil layer.

### 183 3.2. Depth profiles of DO and Eh

184 The depth profiles of DO were monitored on days 0, 3, and 14 (Fig. 3a-c). Prior to the leaf litter amendment,  
 185 all groups exhibited consistent vertical patterns of DO (Fig. 3a). The DO concentration ranged from 3.1 to 3.8  
 186 mg/L in the oxic water layer, gradually declining at the soil-water interfaces. Aerobic conditions were noted at  
 187 20 mm below the soil-water interface (SWI). On day 3, the vertical patterns of DO differentiate in both the LU  
 188 and LC groups, while the DO profiles in the NL group remained relatively unchanged. In both treatment groups,  
 189 the DO concentration in the overlying water decreased, with the LC group exhibiting a slightly higher  
 190 concentration than the LU group (Fig. 2b). Additionally, the gradient in DO profiles became more pronounced,  
 191 with an elevated front of downward-going DO flux. The thickness of the redox transition zone was reduced to  
 192 5 mm and 10 mm in the LU and LC groups, respectively. Similar vertical patterns of DO were observed on day  
 193 14 (Fig. 3c), indicating the persistence of the treatment's effects.

194 The depth profiles of Eh were also monitored on days 0, 3, and 14 (Fig. 3d-f). Before treatment, all groups  
 195 displayed similar vertical Eh patterns (Fig. 3d); the Eh values remained constant at approximately 220 mV in  
 196 the oxic water layer and the top soil layer, and drop roughly -80 mV at 40 mm depth. By day 3, both treatment  
 197 groups exhibited reduced Eh at the water and top soil layers. In the LU group, there was a slight decrease of  
 198 around 30 mV at the interface where the leaf litter was placed, as well as in the upper soil layer. Similar Eh

199 drop at where the leaf litter was placed was also observed in the LC group. On day 14, further decreases in Eh  
 200 values were noted. The LU group experienced an enhanced decline of up to 100 mV in the topsoil layer relative  
 201 to the NL group. In the LC group, the maximum decrease of about 150 mV occurred at 15 mm below the SWI.  
 202 However, the uniformity of the Eh profiles on day 14 within the same group was not as consistent as at earlier  
 203 time points. This variability suggests that the heterogeneity developing in the surface soil layer due to the  
 204 uneven distribution of degraded leaf litter may have influenced the results. Overall, the Eh profiles indicate  
 205 that the surface soil layer quickly became reducing following the addition of leaf litter, with the most  
 206 pronounced effects occurring near the litter material.

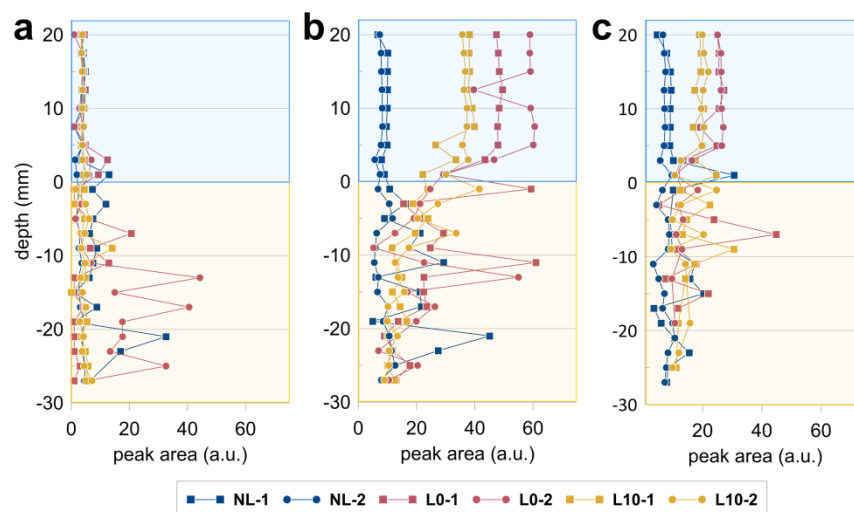


207  
 208 Fig. 3. Spatial distribution of DO and Eh across the soil-water interfaces. Depth profiles of DO on day 0 (a), day  
 209 3 (b), and day 14 (c). Depth profiles of Eh on day 0 (d), day 3 (e), and day 14 (f). The blue and yellow background  
 210 denotes the water column and soil column, respectively. NL = control groups; LU = leaf litter placed at the soil-

211 water interface; LC = leaf litter was covered with a 10-mm-thick soil layer.

### 212 3.3. Depth profiles of fDOM

213 Fluorescent dissolved organic matters (fDOM) levels were measured to represent the degraded products from  
214 leave litter. The depth profiles of fDOM were examined on days 0, 3, and 14 (Fig. 4). Prior to treatment, the  
215 background fluorescence was generally low, with a few exceptions noted in the soil layer deeper than 10 mm  
216 below the sediment-water interfaces (SWIs) (Fig. 4a). Following the addition of leaf litter, there was a rapid  
217 release of fDOM (Fig. 4b) at day 3. In the LU group, fDOM levels in the overlying water rose to between 50 and  
218 60 arbitrary units (a.u.), while the LC group (containing a water overlay, due to the leaf litter settling at the SWI)  
219 experienced an increase of approximately 37 a.u. The variation in fDOM signals suggests that the labile DOM  
220 was rapidly diffused from where leaf litter buried to the overlying top water and the soil layer. By day 14, the  
221 fDOM signal intensity had diminished in both treatment groups where the leaf litter was at the SWI (LO in Fig.  
222 4c) or buried by 10 mm (L10 in Fig. 4c), although it remained significantly higher than that of the control group.  
223 The fDOM signals in the LU and LC groups persisted at around 25 a.u. and 20 a.u., respectively, slightly higher  
224 than the DOM level in the LU group.



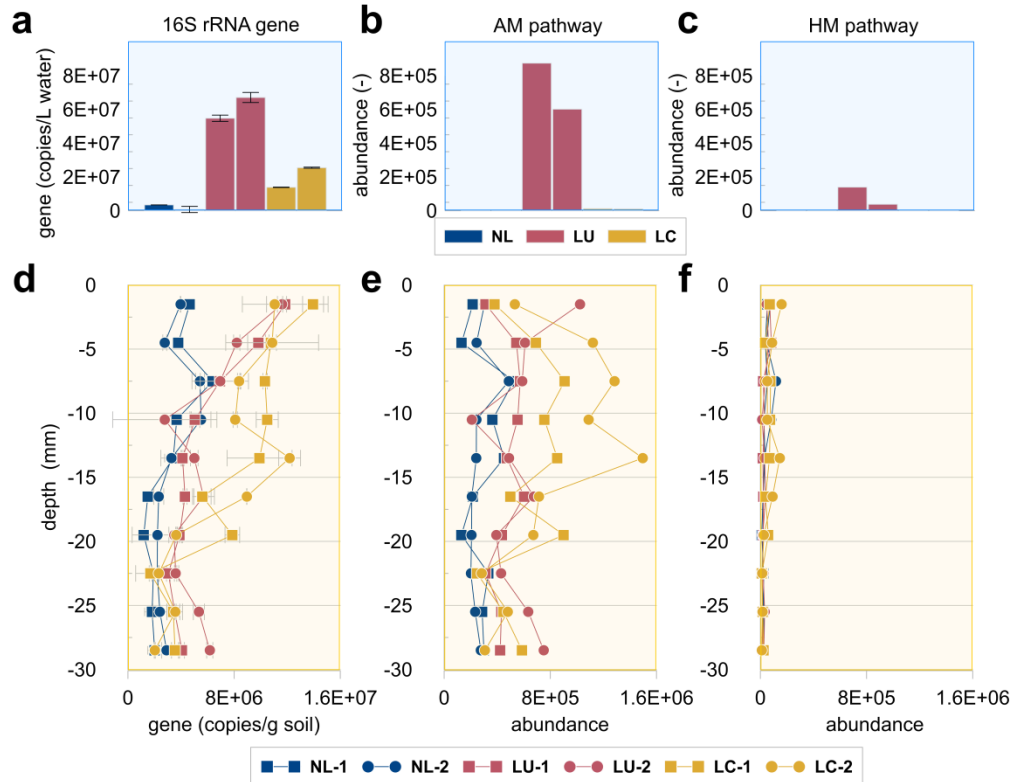
225  
226 Fig. 4. Spatial distribution of fDOM across the soil-water interfaces. Depth profiles of fDOM on day 0 (a), day 3  
227 (b), and day 14 (c). NL = control groups; L0 = leaf litter placed at the soil-water interface; L10 = leaf litter was  
228 covered with a 10-mm-thick soil layer.

229 **3.4 Abundance and distribution of microbial communities**

230 The abundance of microbial organisms along the SWI were measured using 16S rRNA sequencing with  
231 quantitative PCR and displayed in Fig. 5.

232 The addition of leaf litter stimulated the growth of microbial organisms in the water layer and surrounding soil.  
233 In the LU group, the abundance of 16S rRNA gene copies was significantly higher at the top of SWI, reaching  
234  $\sim 1.4 \times 10^7$  copies per gram of soil. This abundance then decreased to levels comparable to the control group at  
235 a depth of about 7.5 mm below the SWI. In the LC group, microbial growth was also enhanced at approximately  
236 13.5 mm below the SWI, where the number of 16S rRNA gene copies was nearly as abundant as at the surface  
237 water.

238 The abundance of the acetoclastic methanogenesis pathway in both the water column and soil column was  
239 depicted in Fig. 5b & 5e, respectively. In the overlying water, the acetoclastic pathway was only detected in the  
240 LU group. In the soil, the LU group and the control group showed similar trends in the abundance of the  
241 acetoclastic pathway. However, the LC group demonstrated a notable increase in the abundance of this  
242 pathway between 10 to 15 mm below the SWI. The abundances of the hydrogenotrophic methanogenesis  
243 pathway were consistently at least one order of magnitude lower compared to the acetoclastic  
244 methanogenesis pathway in both compartments (Fig. 5c & 5f).



245  
 246 Fig. 5. Spatial patterns of microbial communities. 16S rRNA gene copies in water column (a) and soil column (d)  
 247 from technical replicates  $n=3$ ; averages and standard deviation error bars are shown. The predicted pathway  
 248 abundances of acetoclastic methanogenesis in water column (b) and soil column (e). Predicted pathway  
 249 abundance of hydrogenotrophic methanogenesis in water column (c) and soil column (f). AM denotes  
 250 acetoclastic methanogenesis pathway. HM denotes hydrogenotrophic methanogenesis pathway. NL = control  
 251 groups; LU = leaf litter placed at the soil-water interface; LC = leaf litter was covered with a 10-mm-thick soil  
 252 layer.

253 **4. Discussion**

254 **4.1. Distinct patterns in CH<sub>4</sub> and CO<sub>2</sub> emissions**

255 Our findings show that the addition of leaf litter significantly induces CH<sub>4</sub> and CO<sub>2</sub> emissions, but the time-  
 256 dependent variations are distinct with the placement of leaf litter. When leaf litter was placed on the top of  
 257 SWI, the leaf litter was rapid mineralized, resulting in high CO<sub>2</sub> emissions. At the same time, the CH<sub>4</sub> emission  
 258 was enhanced too due to two processes, first, the methane oxidation is inhibited because the diffusion of

259 oxygen to deep soils is blocked (Elberling et al., 2011), as indicated of the Eh profile; second, the labile organic  
260 matter in leaf litter diffused to the deep soils and fueled the acetoclastic methanogens (Fu et al., 2018; Ji et al.,  
261 2018), which is supported by the functional analysis and fDOM profile. Thus, a prolonged methane emission  
262 peak was observed in the LU treatment.

263 When the leaf litter was covered by a thin layer of soil, the soil layer becomes an efficient barrier to slow down  
264 the diffusion of oxygen in the overlying water to the leaf litter (Lorke et al., 2003; Gundersen and Jørgensen,  
265 1990). At the same time, the labile organic matter released during leaf litter degradation diffused upward to  
266 the overlying water layer. Therefore, less but significant CO<sub>2</sub> emission was seen. The addition of leaf litter  
267 stimulated the growth of anaerobic microbial communities, including the methanogens (Nottingham et al.,  
268 2009). The methane emission was high but short-lived, compared to the treatment with leaf litter on the top,  
269 which implies that the supply of organic substrate to the methanogens is hindered in the anaerobic condition.  
270 The prolonged or short-lived methane emission peaks were also observed in other studies. For example, Gong  
271 *et al.*, (2020) investigated the response of methane emissions to litter input in a marsh in two years, and found  
272 a prolonged methane peak in the first year, and a short-lived peak in the second year. The underlying  
273 mechanism of methane emission patterns were usually ignored by other researchers. Our study indicated that  
274 the patterns may be explained by the slight change of litter position during the experiments.

275 Our findings suggest that minor disturbances, on the scale of millimeters, to the place of leaf litter can  
276 substantially alter CH<sub>4</sub> and CO<sub>2</sub> emissions in systems such as wetlands and rice paddies. This raises the  
277 possibility that overlooking the effects of hydrological processes and bioturbation could lead to amplification  
278 of uncertainties in wetland methane budgets and their feedback mechanisms with climate change (Jones et al.,  
279 2020).

#### 280 **4.2. Implications for wetland carbon budget**

281 Although the accumulated CH<sub>4</sub> emission doubled when the leaf litter move from the top of the SWI to 10 mm  
282 below, the GWP20 is lower in the treatment with buried leaf litter, since much less CO<sub>2</sub> was emitted. This



283 finding showed the importance of whole-life analysis of the fate of plant litters.

284 Farmers often supplement the soil with organic matter, mainly straw. This practice enhances soil fertility by  
285 increasing the reservoir of organic matter and essential nutrients for crop growth. However, the strategy of  
286 straw incorporation in paddy systems has sparked debates due to the possible amplification of methane  
287 emissions ensuing from the decay of straw under the anaerobic conditions prevalent in waterlogged rice fields.  
288 Based on the findings, we conclude that burying of plant litters, even with a thin soil layer, can mitigate its  
289 impact on greenhouse emission, at the same time, store more carbon in the anoxic environments. Many  
290 studies showed litter addition, for example, straw returning, induced strong methane emission using the soils  
291 without straw as the control (Ye et al., 2015; Yuan et al., 2018; Jiang et al., 2019). A more reasonable way to  
292 evaluate the consequence of straw returning is to consider the fate of straws, as most of the straws were  
293 eventually transformed to CO<sub>2</sub> or other greenhouse gases through burning, feeding to animals, and/or  
294 composting.

295 Our findings showed that small-scale spatial alternation influences the fate of organic carbon in wetlands. The  
296 existing modeling frameworks usually considered the microbial processes (e.g., methanogens and methane  
297 oxidizers), and the redox-active compounds (e.g., nitrate, sulfate, and organic substrates), in the environment.  
298 Here, we provided evidence showing the geographic patterns, especially the vertical distribution of plant litters  
299 along the redox gradient at SWI, is another vital factors controlling carbon fate. The trade-off between CO<sub>2</sub> and  
300 CH<sub>4</sub> is very sensitive for the leaf litter introduced to SWI. When moving along the depth, leaf litter produce less  
301 CO<sub>2</sub> emissions and more CH<sub>4</sub>, and the ratio may change rapidly at the millimeter scale. Our experiment revealed  
302 that rearranging leaf litter near the soil-water interface can significantly alter the balance of CO<sub>2</sub> and CH<sub>4</sub>  
303 emissions, as well as the GWP20. Therefore, we recommend accounting for the effect of leaf litter placement  
304 on carbon dynamics in modeling scenarios.

## 305 **5. Conclusion**

306 This study provides compelling evidence that millimeter-scale variations in the placement of leaf litter within

307 the SWI of wetlands can significantly impact greenhouse gas emissions, particularly CO<sub>2</sub> and CH<sub>4</sub>. Our  
308 microcosm experiments demonstrated that even minor changes in burial depth can alter the pathways and  
309 rates of organic matter decomposition, leading to considerable differences in gas fluxes. These findings suggest  
310 that existing models of wetland carbon dynamics, which often assume uniform conditions at the SWI, may  
311 overlook critical small-scale heterogeneities that influence carbon cycling and greenhouse gas emissions. The  
312 implications of this research extend to both the scientific understanding of wetland ecosystems and the  
313 strategies employed to mitigate climate change. As wetlands are recognized as key players in global carbon  
314 storage and emissions, accounting for micro-scale variations in leaf litter decomposition could improve the  
315 accuracy of carbon flux predictions and the effectiveness of wetland management practices. Furthermore, this  
316 study highlights the need for high-resolution environmental data and more nuanced modeling approaches that  
317 consider the complexity of natural systems. Future research should focus on exploring the mechanisms driving  
318 the observed effects of leaf litter placement on gas emissions and extending these findings to different types  
319 of wetlands and environmental conditions. By deepening our understanding of these processes, we can better  
320 predict the role of wetlands in the global carbon cycle and develop more informed conservation and  
321 management strategies to harness their potential in mitigating climate change.

#### 322 **Declaration of Competing Interest**

323 The authors declare that they have no known competing financial interests or personal relationships that could  
324 have appeared to influence the work reported in this paper.

#### 325 **Data availability**

326 Data will be made available on request.

#### 327 **Acknowledgments**

328 This work was supported by the National Natural Science Foundation of China (Grant No. 42477116). We  
329 extend our sincere gratitude to Dr. Peng Zhao for his valuable insights into gas flux measurements. We also  
330 thank Ms. Xiao Zhou, Ms. Wen Jiang, Ms. Xiaoping Xie, Ms. Kaidi Tang, and Mr. Yujie Ren for their exceptional

331 technical assistance in the laboratory.

332 **References**

- 333 Barbera, P., Kozlov, A.M., Czech, L., Morel, B., Darriba, D., Flouri, T. and Stamatakis, A. 2019. EPA-ng: Massively  
334 parallel evolutionary placement of genetic sequences. *Syst. Biol.* 68(2), 365-369.  
335 <https://doi.org/10.1093/sysbio/syy054>
- 336 Batson, J., Noe, G.B., Hupp, C.R., Krauss, K.W., Rybicki, N.B. and Schenk, E.R. 2015. Soil greenhouse gas emissions  
337 and carbon budgeting in a short-hydroperiod floodplain wetland. *JGR: Biogeosciences* 120(1), 77-95.  
338 <https://doi.org/10.1002/2014JG002817>
- 339 Battle, J.M. and Golladay, S.W. 2001. Hydroperiod influence on breakdown of leaf litter in cypress-gum wetlands.  
340 *Am. Midl. Nat.* 146(1), 128-145. [https://doi.org/10.1674/0003-0031\(2001\)146\[0128:HI0BOL\]2.0.CO;2](https://doi.org/10.1674/0003-0031(2001)146[0128:HI0BOL]2.0.CO;2)
- 341 Bolyen, E., Rideout, J.R., Dillon, M.R., Bokulich, N.A., Abnet, C.C., Al-Ghalith, G.A., Alexander, H., Alm, E.J., Arumugam,  
342 M., Asnicar, F., Bai, Y., Bisanz, J.E., Bittinger, K., Brejnrod, A., Brislawn, C.J., Brown, C.T., Callahan, B.J.,  
343 Caraballo-Rodríguez, A.M., Chase, J., Cope, E.K., Da Silva, R., Diener, C., Dorrestein, P.C., Douglas, G.M.,  
344 Durall, D.M., Duvallet, C., Edwardson, C.F., Ernst, M., Estaki, M., Fouquier, J., Gauglitz, J.M., Gibbons, S.M.,  
345 Gibson, D.L., Gonzalez, A., Gorlick, K., Guo, J., Hillmann, B., Holmes, S., Holste, H., Huttenhower, C., Huttley,  
346 G.A., Janssen, S., Jarmusch, A.K., Jiang, L.J., Kaehler, B.D., Bin Kang, K., Keefe, C.R., Keim, P., Kelley, S.T.,  
347 Knights, D., Koester, I., Kosciulek, T., Kreps, J., Langille, M.G.I., Lee, J., Ley, R., Liu, Y.X., Loftfield, E., Lozupone,  
348 C., Maher, M., Marotz, C., Martin, B.D., McDonald, D., McIver, L.J., Melnik, A.V., Metcalf, J.L., Morgan, S.C.,  
349 Morton, J.T., Naimey, A.T., Navas-Molina, J.A., Nothias, L.F., Orchanian, S.B., Pearson, T., Peoples, S.L.,  
350 Petras, D., Preuss, M.L., Pruesse, E., Rasmussen, L.B., Rivers, A., Robeson, M.S., Rosenthal, P., Segata, N.,  
351 Shaffer, M., Shiffer, A., Sinha, R., Song, S.J., Spear, J.R., Swafford, A.D., Thompson, L.R., Torres, P.J., Trinh,  
352 P., Tripathi, A., Turnbaugh, P.J., Ul-Hasan, S., van der Hooft, J.J.J., Vargas, F., Vázquez-Baeza, Y., Vogtmann,  
353 E., von Hippel, M., Walters, W., Walters, W., Wan, Y., Wang, M., Warren, J., Weber, K.C., Williamson, C.H.D.,  
354 Willis, A.D., Xu, Z.Z., Zaneveld, J.R., Zhang, Y.L., Zhu, Q.Y., Knight, R. and Caporaso, J.G. 2019. Reproducible,

355 interactive, scalable and extensible microbiome data science using QIIME 2. *Nat. Biotechnol.* 37(9), 1091-  
356 1091. <https://doi.org/10.1038/s41587-019-0209-9>

357 Bridgham, S.D., Cadillo-Quiroz, H., Keller, J.K. and Zhuang, Q. 2013. Methane emissions from wetlands:  
358 biogeochemical, microbial, and modeling perspectives from local to global scales. *Glob. Chang. Biol.* 19(5),  
359 1325-1346. <https://doi.org/10.1111/gcb.12131>

360 Bridgham, S.D., Megonigal, P.J., Keller, J.K., Bliss, N.B. and Trettin, C. 2006. The carbon balance of north American  
361 wetlands. *Wetlands* 26(4), 889-916. [https://doi.org/10.1672/0277-5212\(2006\)26\[889:TCBONA\]2.0.CO;2](https://doi.org/10.1672/0277-5212(2006)26[889:TCBONA]2.0.CO;2)

362 Callahan, B.J., McMurdie, P.J., Rosen, M.J., Han, A.W., Johnson, A.J.A. and Holmes, S.P. 2016. DADA2: High-  
363 resolution sample inference from Illumina amplicon data. *Nat. Methods* 13(7), 581.  
364 <https://doi.org/10.1038/nmeth.3869>

365 Cao, J., He, X., Chen, Y., Chen, Y., Zhang, Y., Yu, S., Zhou, L., Liu, Z., Zhang, C. and Fu, S. 2020. Leaf litter contributes  
366 more to soil organic carbon than fine roots in two 10-year-old subtropical plantations. *Sci. Total. Environ.*  
367 704, 135341. <https://doi.org/10.1016/j.scitotenv.2019.135341>

368 Chiapponi, E., Silvestri, S., Zannoni, D., Antonellini, M. and Giambastiani, B.M.S. 2024. Driving and limiting factors  
369 of CH<sub>4</sub> and CO<sub>2</sub> emissions from coastal brackish-water wetlands in temperate regions. *Biogeosciences* 21(1),  
370 73-91. <https://doi.org/10.5194/bg-21-73-2024>

371 Corteselli, E.M., Burtis, J.C., Heinz, A.K. and Yavitt, J.B. 2017. Leaf litter fuels methanogenesis throughout  
372 decomposition in a forested peatland. *Ecosystems* 20(6), 1217-1232. [https://doi.org/10.1007/s10021-016-](https://doi.org/10.1007/s10021-016-0105-9)  
373 0105-9

374 Ding, W., Cai, Z., Tsuruta, H. and Li, X. 2002. Effect of standing water depth on methane emissions from freshwater  
375 marshes in northeast China. *Atmos. Environ.* 36, 5149–5157. [https://doi.org/10.1016/S1352-](https://doi.org/10.1016/S1352-2310(02)00647-7)  
376 2310(02)00647-7

377 Ding, Y., Wang, D., Zhao, G., Chen, S., Sun, T., Sun, H., Wu, C., Li, Y., Yu, Z., Li, Y. and Chen, Z. 2023. The contribution  
378 of wetland plant litter to soil carbon pool: Decomposition rates and priming effects. *Environ. Res.* 224,  
379 115575. <https://doi.org/10.1016/j.envres.2023.115575>

380 Douglas, G.M., Maffei, V.J., Zaneveld, J.R., Yurgel, S.N., Brown, J.R., Taylor, C.M., Huttenhower, C. and Langille, M.G.I.  
381 2020. PICRUSt2 for prediction of metagenome functions. *Nat. Biotechnol.* 38(6), 685-688.  
382 <https://doi.org/10.1038/s41587-020-0548-6>

383 Dušek, J., Dařenová, E., Pavelka, M. and Marek, M.V. (2020) Climate change and soil interactions, pp. 509-553.

384 Elberling, B., Askaer, L., Jørgensen, C.J., Joensen, H.P., Kühn, M., Glud, R.N., Lauritsen, F.R. 2. Linking Soil O<sub>2</sub>, CO<sub>2</sub>, and  
385 CH<sub>4</sub> Concentrations in a Wetland Soil: Implications for CO<sub>2</sub> and CH<sub>4</sub> Fluxes. *Environ. Sci. Tech.* 45(8), 3393-  
386 3399. <https://doi.org/10.1021/es103540k>

387 Fu, B., Conrad, R., Blaser, M. 2018. Potential contribution of acetogenesis to anaerobic degradation in methanogenic  
388 rice field. soils. *Soil. Biol. Biochem.* 119, 1-10. <https://doi.org/10.1016/j.soilbio.2017.10.034>

389 Galera, L.d.A., Eckhardt, T., Beer, C., Pfeiffer, E.M. and Knoblauch, C. 2023. Ratio of In situ CO<sub>2</sub> to CH<sub>4</sub> production  
390 and its environmental controls in polygonal tundra soils of Samoylov island, northeastern Siberia. *JGR:*  
391 *Biogeosciences* 128(4). <https://doi.org/10.1029/2022JG006956>

392 Glud, R.N., Berg, P., Fossing, H. and Jørgensen, B.B. 2007. Effect of the diffusive boundary layer on benthic  
393 mineralization and O<sub>2</sub> distribution: A theoretical model analysis. *Limnol. Oceanogr.* 52(2), 547-557.  
394 <https://doi.org/10.4319/lo.2007.52.2.0547>

395 Gong, C., Song, C., Sun, L., Zhang, D., Zhang, J. and Liu, X. 2020. Response of methane emissions to litter input  
396 manipulation in a temperate freshwater marsh, Northeast China. *Ecol. Indic.* 115, 106377.  
397 <https://doi.org/10.1016/j.ecolind.2020.106377>

398 Gundersen, J.K., Jørgensen, B.B. 1990. Microstructure of diffusive boundary layers and the oxygen uptake of the sear  
399 floor. *Nature* 345, 604-608. <https://doi.org/10.1038/345604a0>

400 Hu, X., Xie, T., Arif, M., Ding, D., Li, J., Yuan, Z. and Li, C. 2021. Response of annual herbaceous plant leaching and  
401 decomposition to periodic submergence in mega-Reservoirs: Changes in litter nutrients and soil properties  
402 for restoration. *Biology (Basel)* 10(11). <https://doi.org/10.3390/biology10111141>

403 Ji, H., Han, J., Xue, J., Hatten, J.A., Wang, M., Guo, Y. and Li, P. 2020. Soil organic carbon pool and chemical  
404 composition under different types of land use in wetland: Implication for carbon sequestration in wetlands.  
405 *Sci. Total Environ.* 716, 136996. <https://doi.org/10.1016/j.scitotenv.2020.136996>

406 Ji, Y., Liu, P., Conrad, R. 2018. Change of pathway of methane production with progressing anoxic incubation of paddy  
407 soil. *Soil. Biol. Biochem.* 121, 177-184. <https://doi.org/10.1016/j.soilbio.2018.03.014>

408 Jiang, Y., Qian, H.Y., Huang, S., Zhang, X.Y., Wang, L., Zhang, L., Shen, M.X., Xiao, X.P., Chen, F., Zhang, H.L., Lu, C.Y.,  
409 Li, C., Zhang, J., Deng, A.X., van Groenigen, K.J., Zhang, W.J. 2019. Acclimation of methane emissions from  
410 rice paddy fields to straw addition. *Sci Adv* 5, eaau9038. <https://doi.org/10.1126/sciadv.aau9038>

411 Kayranli, B., Scholz, M., Mustafa, A. and Hedmark, Å. 2009. Carbon Storage and Fluxes within Freshwater Wetlands:  
412 a Critical Review. *Wetlands* 30(1), 111-124. <https://doi.org/10.1007/s13157-009-0003-4>

413 Li, W.T., Xu, Z.X., Li, A.M., Wu, W., Zhou, Q. and Wang, J.N. 2013. HPLC/HPSEC-FLD with multi-excitation/emission  
414 scan for EEM interpretation and dissolved organic matter analysis. *Water Res.* 47(3), 1246-1256.  
415 <https://doi.org/10.1016/j.watres.2012.11.040>

416 Liu, X., Lu, X., Yu, R., Sun, H., Xue, H., Qi, Z., Cao, Z., Zhang, Z. and Liu, T. 2021. Greenhouse gases emissions from  
417 riparian wetlands: an example from the Inner Mongolia grassland region in China. *Biogeosciences* 18(17),  
418 4855-4872. <https://doi.org/10.5194/bg-18-4855-2021>

419 Louca, S. and Doebeli, M. 2018. Efficient comparative phylogenetics on large trees. *Bioinformatics* 34(6), 1053-1055.  
420 <https://doi.org/10.1093/bioinformatics/btx701>

421 Lorcker, A., Müller, B., Maerki, M., Wüest, A. 2003. Breathing sediments: The control of diffusive transport across the  
422 sediment-water interface by periodic boundary-layer turbulence. *Limnol. Oceanogr.* 48(6), 2077-2085.  
423 <https://doi.org/10.4319/lo.2003.48.6.2077>

424 Ma, G., Wang, X., Sun, X., Wang, S., Du, Y. and Jiang, J. 2022. Effects of warming and litter positions on litter  
425 decomposition in a boreal peatland. *Front. Eco. Evol.* 10. <https://doi.org/10.3389/fevo.2022.1078104>

426 Mitra, S.W., R.; Vlek, L.G.P. 2005. An appraisal of global wetland area and organic carbon stock. *Curr. Sci.* 88(1), 25-  
427 34. <http://www.jstor.org/stable/24110090>

428 Mitsch, W.J., Bernal, B., Nahlik, A.M., Mander, Ü., Zhang, L., Anderson, C.J., Jørgensen, S.E. and Brix, H. 2012.  
429 Wetlands, carbon, and climate change. *Landscape Ecol.* 28(4), 583-597. [https://doi.org/10.1007/s10980-](https://doi.org/10.1007/s10980-012-9758-8)  
430 [012-9758-8](https://doi.org/10.1007/s10980-012-9758-8)

431 Nahlik, A.M. and Fennessy, M.S. 2016. Carbon storage in US wetlands. *Nat. Commun.* 7, 13835.  
432 <https://doi.org/10.1038/ncomms13835>

433 Neckles, H.A. and Neill, C. 1994. Hydrologic control of litter decomposition in seasonally flooded prairie marshes.  
434 *Hydrobiologia* 286, 155-165. <https://doi.org/10.1007/BF00006247>

435 Neiff, A.P.d., Neiff, J.J. and Casco, S.L. 2006. Leaf litter decomposition In three wetlands types of the Parana river  
436 floodplain. *Wetlands* 26(2), 558-566. [https://doi.org/10.1672/0277-5212\(2006\)26\[558:LLDITW\]2.0.CO;2](https://doi.org/10.1672/0277-5212(2006)26[558:LLDITW]2.0.CO;2)

437 Nilsson, M. and Öquist, M. (2009) Carbon cycling in northern peatlands. Baird, A.J., Belyea, L.R., Reeve, X.C., A.S. and  
438 Slater, L.D. (eds), pp. 131-143.

439 Nottingham, A.T., Griffiths, H., Chamberlain, P.M., Stott, A.W., Tanner, E.V.J. 2009. Soil priming by sugar and leaf-  
440 litter substrates: A link to microbial groups. *Appl. Soil Ecol.* 42, 183-190.  
441 <https://doi.org/10.1016/j.apsoil.2009.03.003>

442 Peng, Y., Zhou, C., Jin, Q., Ji, M., Wang, F., Lai, Q., Shi, R., Xu, X., Chen, L. and Wang, G. 2022. Tidal variation and  
443 litter decomposition co-affect carbon emissions in estuarine wetlands. *Sci. Total Environ.* 839, 156357.  
444 <https://doi.org/10.1016/j.scitotenv.2022.156357>

445 Quast, C., Pruesse, E., Yilmaz, P., Gerken, J., Schweer, T., Yarza, P., Peplies, J. and Glöckner, F.O. 2013. The SILVA  
446 ribosomal RNA gene database project: improved data processing and web-based tools. *Nucleic Acids Res.*  
447 41(D1), D590-D596. <https://doi.org/10.1093/nar/gks1219>

448 Røy, H., Huettel, M. and Jørgensen, B.B. 2004. Transmission of oxygen concentration fluctuations through the  
449 diffusive boundary layer overlying aquatic sediments. *Limnol. Oceanogr.* 49(3), 686-692.  
450 <https://doi.org/10.4319/lo.2004.49.3.0686>

451 Scharlemann, J.P.W., Tanner, E.V.J., Hiederer, R. and Kapos, V. 2014. Global soil carbon: understanding and  
452 managing the largest terrestrial carbon pool. *Carbon Manag.* 5(1), 81-91.  
453 <https://doi.org/10.4155/cmt.13.77>

454 Schiff, S., Aravena, R., Mewhinney, E., Elgood, R., Warner, B., Dillon, P. and Trumbore, S. 1998. Precambrian shield  
455 wetlands: Hydrologic control of the sources and export of dissolved organic matter. *Clim. Change* 40, 167-  
456 188. <https://doi.org/10.1023/A:1005496331593>

457 Stoler, A.B. and Relyea, R.A. 2010. Living in the litter: the influence of tree leaf litter on wetland communities. *Oikos*  
458 120(6), 862-872. doi: 10.1111/j.1600-0706.2010.18625.x

459 Stoler, A.B. and Relyea, R.A. 2013. Bottom-up meets top-down: leaf litter inputs influence predator-prey  
460 interactions in wetlands. *Oecologia* 173(1), 249-257. <https://doi.org/10.1007/s00442-013-2595-x>

461 Watkins, S.C., Nielsen, D., Quinn, G.P. and Gawne, B.E.N. 2011. The influence of leaf litter on zooplankton in  
462 floodplain wetlands: changes resulting from river regulation. *Freshw. Biol.* 56(12), 2432-2447.  
463 <https://doi.org/10.1111/j.1365-2427.2011.02665.x>

464 Xiao, D., Deng, L., Kim, D.G., Huang, C. and Tian, K. 2019. Carbon budgets of wetland ecosystems in China. *Glob.*  
465 *Chang. Biol.* 25(6), 2061-2076. <https://doi.org/10.1111/gcb.14621>

466 Yakimovich, K.M., Emilson, E.J.S., Carson, M.A., Tanentzap, A.J., Basiliko, N. and Mykityczuk, N.C.S. 2018. Plant litter  
467 type dictates microbial communities responsible for greenhouse gas production in amended lake sediments.  
468 *Front. Microbiol.* 9, 2662. <https://doi.org/10.3389/fmicb.2018.02662>

469 Yavitt, J.B. and Williams, C.J. 2015. Linking tree species identity to anaerobic microbial activity in a forested wetland  
470 soil via leaf litter decomposition and leaf carbon fractions. *Plant and Soil* 390(1-2), 293-305.

471 Ye, R.Z., Doane, T.A., Morris, J., Horwath, W.R. 2015. The effect of rice straw on the priming of soil organic matter  
472 and methane production in peat soils. *Soil. Biol. Biochem.* 81, 98-107.  
473 <https://doi.org/10.1016/j.soilbio.2014.11.007>

474 Ye, Y.Z. and Doak, T.G. 2009. A parsimony approach to biological pathway reconstruction Inference for genomes  
475 and metagenomes. *Plos Comput. Biol.* 5(8), e1000465. <https://doi.org/10.1371/journal.pcbi.1000465>

476 Yuan, Q., Hernández, M., Dumont, M.G., Rui, J., Scavino, A.F., Conrad, R. 2018. Soil bacterial community mediates  
477 the effect of plant material on methanogenic composition of soil organic matter. *Soil. Biol. Biochem.* 116,  
478 99-109. <https://doi.org/10.1016/j.soilbio.2017.10.004>

479 Yuan, Z.F., Gustave, W., Bridge, J., Liang, Y., Sekar, R., Boyle, J., Jin, C.Y., Pu, T.Y., Ren, Y.X. and Chen, Z. 2019. Tracing  
480 the dynamic changes of element profiles by novel soil porewater samplers with ultralow disturbance to soil-  
481 water interface. *Environ. Sci. Technol.* 53(9), 5124-5132. <https://doi.org/10.1021/acs.est.8b05390>



482 Zhang, S., Yuan, Z.F., Cai, Y.J., Liu, H., Liu, Z.Y., Chen, Z. 2023. Dissolved solute sampling across an oxic-anoxic soil-  
483 water interface using microdialysis profilers. JoVE 193, e64358. <https://dx.doi.org/10.3791/64358>

484

**Declaration of interests**

The authors declare that they have no known competing financial interests or personal relationships that could have appeared to influence the work reported in this paper.

The authors declare the following financial interests/personal relationships which may be considered as potential competing interests: